Phys. Status Solidi A **209,** No. 9, 1721–1725 (2012) / **DOI** 10.1002/pssa.201200057

physica status solidi a
www.pss-a.com
applications and materials science

Part of Topical Section on
Fundamentals and Applications of Diamond

Direct nanopatterning of commercially pure titanium with ultra-nanocrystalline diamond stamps

A. I. M. Greer*, K. Seunarine, A. Z. Khokhar, X. Li, D. A. J. Moran, and N. Gadegaard

School of Engineering, Rankine Building, University of Glasgow, Glasgow G12 8QQ, UK

Received 16 April 2012, revised 1 June 2012, accepted 3 June 2012
Published online 31 July 2012

Keywords diamond, imprint, nanotopography, titanium

*Corresponding author: e-mail a.greer.1@research.gla.ac.uk, Phone: +44 141 330 2000 (ext 5243), Fax: +44 141 330 4907

In order to directly imprint features into a hard metal such as titanium, an imprinting stamp composed of material of greater hardness is required. Diamond is the hardest known material, so is an obvious choice for the production of direct-imprint stamps. Diamond also benefits from a low surface energy, chemical inertness, high resistance to wear and is easily cleaned of contaminants, further favouring it as a stamp material of choice. Chemical vapour deposited ultra-nanocrystalline diamond (UNCD) provides similar mechanical properties to bulk single crystal diamond and can be deposited across large surface areas. This work examines the use of UNCD as a stamp medium for the transfer of nanoscale features into commercially pure titanium (cpTi) substrates. Development of an efficient and viable method for nanopatterning large, non-planar cpTi surfaces is highly desirable to control cell adhesion on the surface of bio-implants. The fabrication of UNCD nanoimprint stamps is detailed and the ability of UNCD to imprint cpTi is illustrated. A square-ordered matrix of 200 nm diameter pillars over a quarter mm square area are shown to be imprinted with the depth quantified against load (kg). The limitations of the technology are also discussed.

1 Introduction Commercially pure titanium (cpTi) is widely used in dental and orthopaedic implants. The surface texture of such implants has also been shown to influence cell adhesion [1, 2]. The ability to accurately control cell adhesion to implants is important as it could eliminate the use of short-life cement for permanent implants and prevent unwanted cell growth on temporary implants. To date, the majority of this research has been carried out using polymer substrates [1, 2]. In order to implement the results of the polymer research onto titanium-based implants, a method first needs to be developed for efficiently defining the required topographies on titanium.

Modification of cpTi surfaces is often carried out using coatings, such as calcium phosphate [3], or by introducing surface roughness, typically by electro-polishing or sand blasting [4]. One of the main disadvantages of using these techniques is that they only allow a limited control of the surface features shape, size and density as well as surface roughness. These factors can be controlled to a greater extent by using methods derived from the microelectronics industry. However, for bio-implant applications, large area (mm/cm scale) and non-planar surfaces need to be patterned. Conventional processing such as plasma, ion or e-beam patterning and evaporation of materials or etching are difficult to implement under these conditions. An alternative method to address this requirement of pattern transfer into cpTi is direct imprinting.

CpTi is a hard material (Young's modulus of 105 GPa [5]) and therefore requires a material of greater hardness to imprint directly into it. Diamond is an ideal candidate as it is an order of magnitude harder (1050 GPa [6]), has high resistance to wear [7] (long life time), can be terminated to inhibit adhesion [8] (easing extraction from the stamped media), requires extremely high temperatures to expand [9] (eliminating stamp deformity problems for high friction processing), is chemically inert (for stamp minimal feature degradation when cleaned) and can be etched with good resolution [10]. For these reasons diamond has already been utilised for imprinting applications. In particular, single crystal diamond has been used on the tip of nanoindentation machines and more recently on atomic force microscope (AFM) tips [11]. Chemical vapour deposited (CVD) diamond has been

the focus of several imprint experiments for soft materials [12] largely because the wetting angle of diamond can be tailored in the range of 5–106° [13]. For angles approaching 106° the surface energy is considered low. A low surface energy means that the material repels adhesives which is particularly important for imprinting molten materials where otherwise chemical reactions may cause diffusion and bonding of ions at the interface [13]. The surface energy is dependent on termination chemistry. Termination with hydrogen is known to provide a low surface energy for diamond [8] and since hydrogen gas is present during conventional CVD growth, the diamond produced is often found to be hydrogen terminated [14, 15]. Guo et al. [16] have reported that a reduction in surface energy decreases adhesion and interface strength between diamond and metal, therefore (as-grown) hydrogen terminated diamond is beneficial to the imprint process. To date there are few examples of direct nanoimprinting of metal with diamond. Beyond controlling cell interaction, direct pattern transfer via imprinting finds application in various technologies including circuit definition [12], optical devices [17] and mass storage media [18]. The documented examples of direct nanopatterning at present were performed on soft metals or thin films above soft substrates as opposed to the hard, bulk metal considered in this study. For thin metal films, silicon based stamps have thus far proved sufficient for this task. In 2002 Taniguchi et al. [12] demonstrated the ability to directly pattern bulk aluminium and copper with single crystal diamond, producing 100 and 50 nm deep features, respectively, from a 270 nm deep, 1 μm wide stamp. In 2003 Lister et al. [10] published similar work achieving a direct imprint into nickel with sub-10 nm gratings, 40 nm pitch and unconfirmed depth. In 2004 Yoshino et al. nanopatterned 300 nm diameter pillars into both bulk aluminium [19] and hard non-metal materials [20], again using single crystal diamond.

Definition of the diamond stamp features is typically achieved through electron-beam lithography and oxygen based reactive ion etching. Oxygen has been used for plasma-assisted ion etching since 1990 [21] and is now a reliable and well-established process for structuring diamond. Diamond can also be masked with a range of materials [22] allowing versatile processing. In recent years mask-free feature fabrication has been demonstrated by Yang at al [23], who reported on the use of incorporated impurities as masks in 2008.

In contrast to the reported work utilising single crystal diamond substrates, in this work we report on the use of ultra-nanocrystalline diamond (UNCD) material for the fabrication of stamps for direct-imprinting into titanium.

2 Materials and methods

2.1 Materials The UNCD used for this work was commercially sourced and consisted of a 1.85 μm film of CVD diamond grown on a 4 in., 530 μm thick, ⟨100⟩ silicon wafer. The UNCD film comprised of diamond grains 3–5 nm in diameter with atomically abrupt boundaries, and a typical root-mean-squared surface roughness of 10–20 nm [24].

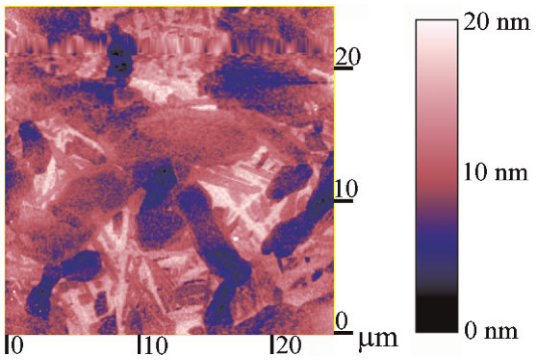

Figure 1 (online colour at: www.pss-a.com) AFM 25 μm square scan of cpTi surface after polishing. Image $R_a = 2.352$ nm.

UNCD is reported to have excellent mechanical properties [25], including a comparable Young's modulus to that of bulk diamond (~850 GPa [24]) yet is cheaper than single crystal diamond, can cover much larger areas and can be grown on to three-dimensional surfaces [26]. All of these factors are important in creating an efficient imprint process.

The titanium material used for imprinting was commercially sourced as a 3 m rod of diameter 10 mm. It was sliced into 6 mm thick disks and the flat surfaces polished using a Bheuler Motopol 2000 chemical–mechanical grinding and polishing tool. Emery paper was used for the first four grinding stages with sequentially decreasing grit size. This was followed by polishing with 1 μm grain diamond slurry on a Kemet International Chem-H polishing pad. For the final stage the abrasive was switched to colloidal silica. It was discovered that the addition of hydrogen peroxide (3%) to the colloidal silica stage is beneficial for minimising surface roughness. Polishing with a hydrogen peroxide mix of ~1:5/H_2O_2:colloidal silica is recommended but the duration should be restricted to 40 min because longer periods result in pits forming on the cpTi surface. A mirror finish of sub 3 nm (arithmetic average) roughness was achieved using the above method, as shown on the AFM scan in Fig. 1.

2.2 Imprint stamp fabrication The UNCD samples were first exposed to acid (SC-1) and solvent cleaning after which 2 nm of titanium was electron-beam evaporated onto the surface to act as a resist adhesion promoter. Hydrogen silsesquioxane (HSQ) negative resist was then spun onto the samples to obtain an ~100 nm thick film. The sample was then immediately baked on a hotplate for 2 min at 90 °C to allow good (sub-10 nm [10]) lithography resolution. Following the hotplate bake, 15 nm of aluminium was evaporated onto the surface of the resist to act as a charge dissipation layer (CDL) and minimise feature distortion due to surface charging during electron beam lithography [27]. The HSQ was then exposed using a Vistec Vector Beam 6 electron beam lithography tool. Each design was a square matrix of side 250 μm consisting of 200 nm diameter circular features at 560 nm pitch to emulate topographies previously

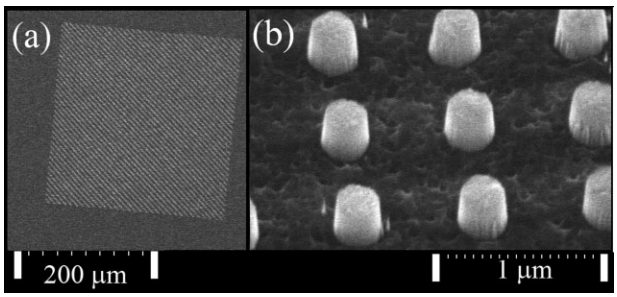

Figure 2 (a) SEM over-view image of a pillar matrix stamp etched into UNCD with side 250 μm consisting of 200 nm diameter circular pillars at 560 nm pitch. (b) Close-up SEM image of 200 nm pillars at 45 degree tilt.

constructed for our cell work on polymer substrates [1]. After exposure, the 15 nm aluminium CDL was removed by manually agitating the sample in aluminium etch (5% nitric acid, 15% reverse osmosis water and 80% orthophosphoric acid) for 1 min. The HSQ patterns were developed in tetramethylammonium hydroxide (TMAH), after which the titanium adhesion promotion layer was removed by reactive ion etching using SF_6. Although this chemistry also etches HSQ, the short etch duration ensures minimal degradation of the HSQ features. Once the non-patterned areas were free from Ti, the diamond was etched using $Ar : O_2 = 10$ sccm: 40 sccm, at 200 W, 20 mT with DC bias 518 V for 5 min. This recipe has a diamond: HSQ etch ratio of ~2:1. Figure 2 shows images from a scanning electron microscope (SEM) of 200 nm diameter UNCD features etched using the above process. The depth of the diamond features was measured using an AFM, a cross-sectional profile from which is shown in Fig. 3.

2.3 Imprinting After fabricating the UNCD stamps, they were pressed into the polished cpTi using a manual, hydraulic press. Stamps were embossed at a range of loads between 100 and 750 kg. A hold period of 30 s was applied at peak load for each imprint. Even imprint pressure distribution was ensured by the incorporation of 5 mm thick tungsten carbide/cobalt (Young's modulus 600 GPa) plates on the press bolsters. The cpTi was then re-examined for topographical alterations by AFM and SEM analysis.

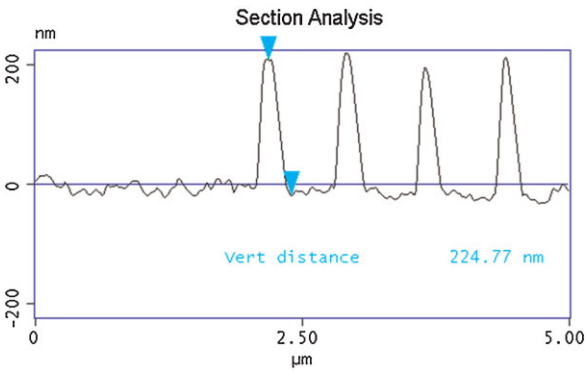

Figure 3 (online colour at: www.pss-a.com) AFM section analysis of a 200 nm diameter stamp, the vertical distance between the two arrows and hence height of the features is shown to be ~225 nm.

3 Results The inverse of the stamp profile was transferred into the cpTi via the imprinting process resulting in the formation of an array of holes on the titanium surface (Fig. 4 shows an SEM image of imprinted cpTi sample). The perimeter features were the first to be transferred. The imprint depth was measured near the pattern perimeter with AFM and confirmed with transmission electron microscopy (TEM). In order to perform TEM analysis, a focused ion beam (FIB) was used to cut a cross-section from the imprinted cpTi. To protect the cpTi surface during this procedure the sample was first covered in Pt. Two separate Pt depositions were used to create the protective barrier. The first deposition was electron beam induced which, although does not have as high a deposition rate, is reported to produce less damage to the surface than ion beam deposition [28]. Ion beam deposition was then used to build up the thickness of the protective Pt layer. A TEM image of one of the imprint sites is shown in Fig. 5.

The depth of imprint features was recorded against applied load, the results of which are displayed in Fig. 6. The nonlinear contour can be explained by the decreasing space between the stamp base and cpTi surface because it restricts the movement of the displacing cpTi pile-up effect. Pei et al. [29] have modelled the nanopatterning of metal and concluded this result was to be expected. They also suggest that the build-up of dislocations beneath the metal surface may contribute to the contour shape as a result of a work-hardening effect.

4 Discussion The work by Pei et al. [29], previously mentioned in Section 3, details the molecular simulation of direct nanoimprinting of copper. Although this study is not based on cpTi, it does give some indication of the behaviour of a crystalline metal under similar conditions to the work

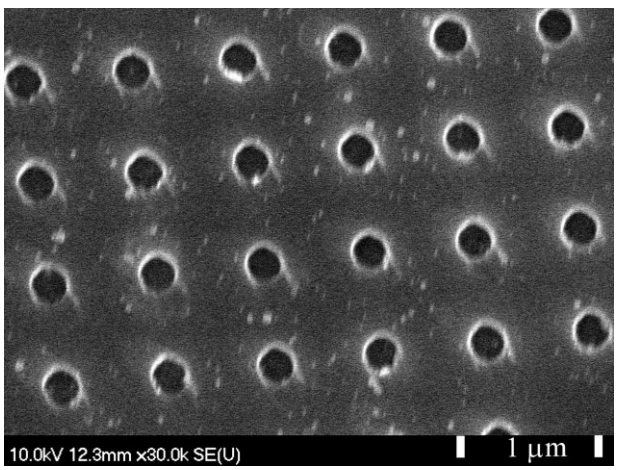

Figure 4 SEM image of cpTi surface following imprinting using a UNCD stamp with 200 nm diameter features and a load of 200 kg.

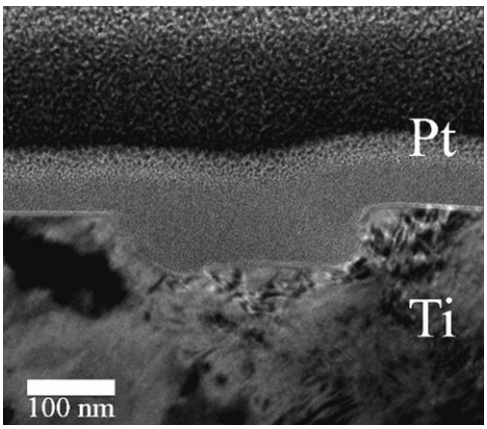

Figure 5 TEM cross-section image of a single feature site on cpTi after imprinting with a UNCD stamp of feature diameter 200 nm at a load of 100 kg. The imprint is 50 nm deep and the Ti is covered with Pt for protection. The Pt was deposited with two separate induction beams which has produced two visually distinct layers.

presented here. The detailed analysis includes emphasis on the effect of the interaction of stress fields in the substrate when the stamp has closely spaced features. They report that work hardening due to the build-up of dislocations will result in larger loads being required for imprinting set depths. This principal explains why the features comprising the perimeter of the stamp are the first to cause plastic deformation. The entire stamp profile was transferred once the load was increased beyond 300 kg.

The part of the system most susceptible to mechanical failure is the silicon substrate on which the UNCD is grown. Once the stamp features are fully embedded in the cpTi, the entire stamp substrate begins to act as the contact area. Thus much higher loads are required to produce plastic deformity

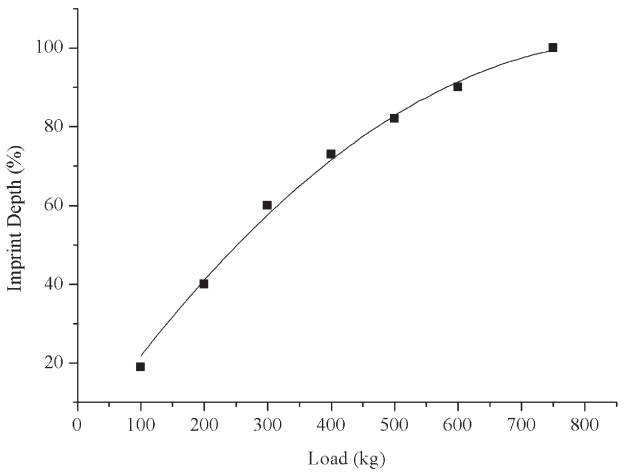

Figure 6 Graph of imprint depth against applied pressing load for a UNCD stamp of side 250 μm containing 200 nm diameter circular pillars with 560 nm pitch into polished, planar cpTi. The depth is measured as a percentage with reference to feature height (100% = 225 nm).

in the cpTi beyond this point. Increasing the load beyond 750 kg always resulted in the silicon substrate cracking as it is unable to handle such a high level of stress. Damage to the silicon substrate often precipitates into the diamond layer. To ensure reusability, the stamp profiles should therefore be designed with 'higher' features than the designated imprint depth. It is recommended from our findings that stamp features should have 20% additional height than the desired imprint depth. Alternatively, use of a harder substrate material to support the UNCD layer such as SiC could be considered.

During imprinting the UNCD features displace a relative volume of cpTi. The cpTi displaces in a radial direction from the centre and the volume of displacing material increases towards the outer edges of the stamp. The embedded UNCD features around the edge experience the most perpendicular stress from this flow. For loads of 600 kg and above this stress was sufficient to shear the features around the edges of the stamp. As the load is increased the volume of displaced material is increased and the flow space between the surfaces is reduced resulting in increased perpendicular stress which subsequently fractures more of the perimeter features.

5 Conclusions We have shown that thin film UNCD on Si has sufficient stiffness and compressive strength to be utilised as a stamp material for pattern transfer into a hard, bulk metal such as Ti, through direct imprinting. We have demonstrated that feature sizes as small as 200 nm can be successfully transferred to depths of a similar dimension and believe that sub-200 nm should be obtainable utilising this process. However, it is acknowledged that there is an optimum load for imprinting a stamp with the profile considered here. Since a load greater than 300 kg is required before features in the central area of the stamp begin to transfer into the cpTi, and loads of 600 kg and above result in feature shearing at the edges of the stamp, 350–550 kg is concluded to be the optimum loading range in this instance. This window restricts the obtainable feature depth to ~125–190 nm. However, the main advantage UNCD has over single crystal diamond is that it can be grown over large area, non-planar surfaces. It is therefore anticipated that a roller embossing tool with a UNCD surface coating could avoid the load limitations discussed here. Since the contact area of a roller will be a tangential section the load required for imprinting set depths will be lower and imprint uniformity issues will be minimised. The displacing material would also be decreased so perpendicular stresses would be lower and thus the probability of feature shearing due to pile-up displacement would be less.

6 Future work This work is continuing to examine the impact of surface oxide on the imprint behaviour. Experimentation is also being carried out on the transfer of UNCD features to cpTi between a curved and planar surface to determine whether UNCD may work effectively as a roller imprint coating for this application.

Acknowledgements This work was funded by the EPSRC and supported by NaPANIL (FP7-CP-IP 214249-2). A processing was carried out in the James Watt Nanofabrication Centre (JWNC) at The University of Glasgow. We are grateful for the support and training provided by the JWNC technical staff. We would also like to acknowledge the valuable contributions from Billy Smith and Colin How for their operation of the FIB and TEM.

References

[1] N. Gadegaard, M. J. Dalby, M. O. Riehle, and C. D. W. Wilkinson, J. Vac. Sci. Technol. B **26**, 2554–2557 (2008).
[2] M. J. Dalby, N. Gadegaard, R. Tare, A. Andar, M. O. Riehle, P. Herzyk, C. D. W. Wilkinson, and R. O. C. Oreffo, Nature Mater. **6**, 997–1003 (2007).
[3] C. Chen, I. S. Lee, S. M. Zhang, and H. C. Yang, Acta Biomater. **6**, 2274–2281 (2010).
[4] S. P. Xavier, P. S. P. Carvalho, M. M. Beloti, and A. L. Rosa, J. Dentistry **31**, 173–180 (2003).
[5] K. Zhu, C. Li, Z. Zhu, and C. Liu, J. Mater. Sci. **42**, 7348–7353 (2007).
[6] N. Savvides and T. Bell, J. Appl. Phys. **72**, 2791–2796 (1992).
[7] S. Bull, Diam. Relat. Mater. **4**, 827–836 (1995).
[8] L. Ostrovskaya, V. Perevertailo, V. Ralchenko, A. Dementjev, and O. Loginova, Diam. Relat. Mater. **11**, 845–850 (2002).
[9] D. Gibbons, Phys. Rev. **112**, 136 (1958).
[10] K. Lister, S. Thoms, D. Macintyre, C. Wilkinson, J. Weaver, and B. Casey, J. Vac. Sci. Technol. B **22**, 3257 (2004).
[11] J. W. Park, D. W. Lee, N. Takano, and N. Morita, Mater. Sci. Forum. **505**, 79–84 (2006).
[12] J. Taniguchi, Y. Tokano, I. Miyamoto, M. Komuro, and H. Hiroshima, Nanotechnology **13**, 592 (2002).
[13] L. Ostrovskaya, V. Perevertailo, V. Ralchenko, A. Saveliev, and V. Zhuravlev, Diam. Relat. Mater. **16**, 2109–2113 (2007).
[14] L. Yang, Y. Li, B. W. Sheldon, and T. J. Webster, J. Mater. Chem. **22**, 205–214 (2011).
[15] H. Kawarada, Surf. Sci. Rep. **26**, 205–259 (1996).
[16] H. Guo, Y. Qi, and X. Li, J. Appl. Phys. **107**, 033722–033728 (2010).
[17] S. Pang, T. Tamamura, M. Nakao, A. Ozawa, and H. Masuda, J. Vac. Sci. Technol. B **16**, 1145 (1998).
[18] Y. Hirai, T. Ushiro, T. Kanakugi, and T. Matsuura, Proc. SPIE **5220**, 74 (2003).
[19] W. Kurnia and M. Yoshino, J. Micromech. Microeng. **19**, 125028 (2009).
[20] M. Yoshino and S. Aravindan, J. Manuf. Sci. Eng. **126**, 760 (2004).
[21] A. B. Harker and J. F. DeNatale, J. Mater. Res. **5**, 818–823 (1990).
[22] D. Tran, C. Fansler, T. Grotjohn, D. Reinhard, and J. Asmussen, Diam. Relat. Mater. **19**, 778–782 (2010).
[23] N. Yang, H. Uetsuka, E. Osawa, and C. E. Nebel, Nano Lett. **8**, 3572–3576 (2008).
[24] Advanced diamond technologies incorporated, UNCD Wafers: Advanced Diamond Technologies Data Sheet & Technical Knowledge Bank, www.thindiamond.com (2010).
[25] J. Narayan, Mater. Sci. Eng. B **25**(1), 5–10 (1994).
[26] M. Bonnauron, S. Saada, C. Mer, C. Gesset, O. A. Williams, L. Rousseau, E. Scorsone, P. Mailley, M. Nesladek, and J. C. Arnault, Phys. Status Solidi A **205**(9), 2126–2129 (2008).
[27] A. I. M. Greer and D. A. J. Moran, Diam. Relat. Mater. (2012); DOI: 10.1016/j.diamond.2012.07.003.
[28] W. Y. Kwong and W. Y. Zhang, Proc. IEEE International Symposium on Semiconductor Manufacturing (ISSM 2005), 2005, pp. 469–471.
[29] Q. Pei, C. Lu, Z. S. Liu, and K. Y. Lam, J. Phys. D **40**, 4928 (2007).